



# Compound precipitation and wind extremes over Europe and their relationship to extratropical cyclones

Laura E. Owen<sup>a,\*</sup>, Jennifer L. Catto<sup>a</sup>, David B. Stephenson<sup>a</sup>, Nick J. Dunstone<sup>b</sup>

<sup>a</sup> College of Engineering, Mathematics and Physical Sciences, The University of Exeter, UK

<sup>b</sup> Met Office, Exeter, UK

## ARTICLE INFO

### Keywords:

Compound extremes

Winds

Precipitation

Extratropical cyclones

## ABSTRACT

Extratropical cyclones and their associated extreme precipitation and winds can have a severe impact on society and the co-occurrence between the two extremes is important when assessing risk. In this study the extremal dependency measure,  $\chi$ , is used to quantify the co-occurrence of extreme precipitation and wind gusts, and is investigated at individual grid points and spatially over Europe. Results using three observational datasets and a higher spatial and temporal resolution version of ERA5 than previously used confirm previous studies. Over Europe high co-occurrence is found over western coasts and low co-occurrence is found over eastern coasts. All datasets have qualitatively similar spatial patterns over most regions of Europe excluding some regions of high topography where ERA5  $\chi$  values are much larger. ERA5 represents the timings of daily extreme co-occurring events well, compared to observations. The differences in precipitation accumulation timescales are also accounted for by considering hourly, 6, 24 and 48 hourly co-occurrence. In a few regions co-occurrence changes with longer accumulations, indicating the different speeds and sizes of weather systems affecting these regions.  $\chi$  in most regions has little increase by allowing a 24 h lag and lead between the precipitation and wind, with a few exceptions where  $\chi$  is increased by up to 24%. Regions with the larger of these increases are on or around elevated topography. Using an objective feature tracking method, insight into the spatial pattern of extreme precipitation and wind within cyclones over Europe is given. As well as suggesting how many hours apart the extremes occur from one another in a particular location. Extreme co-occurring events are associated with cyclones far more of the time than non extreme events. Given an extreme co-occurring event the chance of a cyclone being within 1110 km is more than 70% for much of Europe. Regions with low co-occurrence have extremes caused by different weather systems and regions with large co-occurrence have both extremes caused by the same weather system. Cyclones linked to extreme events, particularly co-occurring and extreme wind, have larger intensity than those not and for most of Europe these cyclones also have faster mean speed.

## 1. Introduction

Strong winds caused by extratropical cyclones are capable of producing devastating socio-economic impacts over Europe (Roberts et al., 2014). Storm Kyrill, for example, caused considerable damage, with estimated insured losses for Europe of £6.3 billion (Fink et al., 2009; Swiss Re, 2000). Precipitation extremes and associated floods can also have a major impact and cause huge socioeconomic loss (Easterling et al., 2000; Pall et al., 2011). For example, the 2013/14 winter UK floods caused economic damages of £1.3 billion (Environmental Agency, 2016). Compound effects of multiple drivers, such as precipitation and wind together, cause the majority of weather and climate related catastrophes (Zscheischler et al., 2018). The co-occurrence of extreme precipitation and winds can have a severe impact on society

and this co-occurrence is important when assessing risk since together they can cause even greater damage than separately. This could provide useful information for the (re)insurance industry and emergency response planners.

Martius et al. (2016) quantified the global co-occurrence of daily precipitation and wind extremes using ERA-Interim precipitation and wind gust data from 1979 to 2012, by calculating the extremal dependency measure,  $\chi$ . The co-occurrence of wind and precipitation extremes (above the 98th percentile) were defined by events occurring at the same gridpoint on the same day or shifted in time by one day. For winter (December to January) high percentages of co-occurring extremes were along the west coast of Spain and Portugal, northwestern central Europe, the west coast of Norway and the east coast of Greece.

\* Corresponding author.

E-mail address: [lb663@exeter.ac.uk](mailto:lb663@exeter.ac.uk) (L.E. Owen).

<https://doi.org/10.1016/j.wace.2021.100342>

Received 21 July 2020; Received in revised form 30 March 2021; Accepted 24 June 2021

Available online 6 July 2021

2212-0947/Crown Copyright © 2021 Published by Elsevier B.V. This is an open access article under the Open Government License (OGL)

(<http://www.nationalarchives.gov.uk/doc/open-government-licence/version/3/>).

Lowest co-occurrences were in eastern Norway and Sweden, eastern Spain and eastern central Europe.

It is important to consider whether the results of [Martius et al. \(2016\)](#) are robust to different datasets. For example, there are uncertainties since ERA-Interim precipitation and wind data are model derived from short term forecasts and are not constrained by observations. [Pfahl and Wernli \(2012\)](#) did compare ERA-Interim with satellite observation based precipitation data. The magnitude of precipitation intensity agreed well for Europe and more importantly the timing of 6 hourly extreme precipitation matched more than 80% of the time for most of Europe. Nevertheless, extreme precipitation events were not systematically evaluated in the satellite dataset used and uncertainties were largely unknown. Therefore, a similar study using observational datasets to test spatial patterns of extreme precipitation and wind as well as the timings of the extreme co-occurring events is needed. Although a full validation using such datasets is impossible since observational datasets are limited due to sparse stations resulting in missing data in space and time as well as low temporal resolutions.

There is statistical evidence of a time separation between flooding and extreme wind over Great Britain, where peak river flows occur 0 to 13 days after extreme wind ([De Luca et al., 2017](#)). Over the Mediterranean, [Raveh-Rubin and Wernli \(2015\)](#) found that the timing of the precipitation peak typically occurred 12 h before the gust peak. From five case studies of cyclones in the Mediterranean, [Raveh-Rubin and Wernli \(2016\)](#) found that spatial distributions of extreme wind gusts and precipitation are largely separated, with limited overlap. Extreme wind gusts occurred in the south western parts of a cyclone while precipitation had localized peaks, which varied from case to case. The peak in precipitation occurred at the same time as the deepest minimum in sea level pressure and the wind gust followed within the next 6 h ([Raveh-Rubin and Wernli, 2016](#)). However it is still unknown about the climatological separation between extreme precipitation and wind throughout Europe.

Many papers have looked at the relationship between extratropical cyclones and their associated fronts and extreme precipitation ([Pfahl and Wernli, 2012](#); [Hawcroft et al., 2012](#); [Catto and Pfahl, 2013](#)). Whilst other papers have looked at the relationship between extratropical cyclones and their associated fronts and extreme winds ([Roberts et al., 2014](#); [Hewson and Neu, 2015](#)). However few papers have looked at the relationship between extratropical cyclones and co-occurring precipitation and wind extremes. Over Great Britain extreme winter wind and precipitation co-occur and are linked by the physical processes associated with extratropical cyclones ([De Luca et al., 2017](#)). Large co-occurrence over the Northwest of the Alps, is explained by the fact extreme wind and precipitation events over this region are typically associated with cyclones over the North Sea ([Martius et al., 2016](#); [Pfahl, 2014](#)). Alternatively to the east of the Alps a lower co-occurrence was found ([Martius et al., 2016](#)), extreme precipitation in this region is caused by Mediterranean cyclones, however wind extremes in this region are caused by cyclones from northern Europe ([Martius et al., 2016](#); [Pfahl, 2014](#)). This suggests that low co-occurrence occurs in regions where the extremes come from different weather systems. [Martius et al. \(2016\)](#) also suggested that regional variations in co-occurring extremes are due to the location of cyclone centres in relation to these extremes. Over the Mediterranean these combined extremes often occur simultaneously near North Atlantic cyclones or Mediterranean cyclones ([Raveh-Rubin and Wernli, 2015](#)).

Some work has looked at the characteristics; speed and latitudinal displacement of cyclones causing extreme precipitation ([Pfahl, 2014](#)), however the same study for cyclones causing both precipitation and wind extremes has not been done, nor for other cyclone characteristics.

Until now there has been little published literature on the co-occurrence of precipitation and wind extremes over Europe, and in particular linking these extremes to extratropical cyclones. This study quantifies the co-occurrence of extreme precipitation and wind over Europe, building upon [Martius et al. \(2016\)](#). This study expands on [Martius et al. \(2016\)](#) by using ERA5 data which has a higher spatial

and temporal resolution to ERA-Interim, as well as three observational datasets, to explore the robustness of the results. Due to the higher temporal resolution of ERA5, hourly data was used to investigate co-occurrence, meaning differences in  $\chi$  due to the temporal scale of the precipitation extremes have been investigated. This is useful because precipitation characteristics are different depending on the timescale and location ([Barbero et al., 2019](#)). We might also expect different co-occurrence for different precipitation accumulation periods because of the weather systems causing the extreme precipitation and wind. In previous studies the time separation between precipitation and wind extremes was only investigated for the Mediterranean and for a small number of cases. In this study the time separation has been quantified for the whole of Europe with a much larger sample size. An objective feature tracking algorithm was used to find cyclones and investigate the probability of a cyclone given an extreme co-occurring event, this was also quantified for all of Europe. Cyclone speed and intensity was investigated to see whether extreme co-occurring events have preferred cyclone characteristics. The extended winter season (October to March) was used because many extreme events due to storms occur in the autumn and spring seasons in Europe, hence when assessing cyclone related risk these are the months of interest. Extremes in this study were taken as above the 80th and 99th percentiles (see Section 2.2 for detail). The following questions are addressed:

1. What is the spatial distribution of the probability of co-occurrence of extreme precipitation and extreme winds over Europe in the reanalysis and observational datasets?
2. How does the temporal scale of the precipitation extremes affect the co-occurrence?
3. Can we quantify the temporal offset of the extreme precipitation and winds over Europe?
4. How strongly related are the co-occurrence of extremes to extratropical cyclones and are there preferred cyclone characteristics?

## 2. Data and methodology

### 2.1. Data

Hourly total precipitation accumulation and 10 m wind gust since previous post-processing from the European Centre for Medium-range Weather Forecasts ERA5 reanalysis dataset are used ([Hersbach et al., 2020](#)). Other time periods, 6, 24 and 48 h, are the accumulated precipitation and maximum wind gust within that timeframe. The ERA5 dataset is a global dataset with spatial resolution of 31 km (0.28125°). Both the ERA5 precipitation and wind gust data are from forecasts.

To check the robustness of the ERA5 dataset results, two observational station datasets are used; NOAA's National Climatic Data Center's, Global Surface Summary Of the Day (GSOD) dataset, and the European Climate Assessment (ECA) dataset. GSOD is comprised of daily data computed from global hourly station data ([National Climatic Data Center, 2018](#)). The ECA dataset contains series of daily observations at meteorological stations throughout Europe and the Mediterranean ([Van Den Besselaar et al., 2015](#)). From both the GSOD and ECA datasets daily precipitation accumulation and daily maximum wind gusts are used from 825 and 805 European stations respectively. Precipitation and maximum wind gust will only appear if the station reports the data sufficiently to provide a valid value. Therefore, many days have missing values. Stations with limited wind gust and precipitation data (less than 1% of the total number of timesteps) are removed in this analysis. The gridded version of the ECA daily precipitation dataset, E-OBS, is also used to check robustness. E-OBS comes as an ensemble dataset and is downloaded on a 0.25° regular grid for daily precipitation sum. The ensemble mean is used as this is provided as the 'best-guess' ([Cornes et al., 2018](#)). A new dataset is created, E-OBS/ERA5 with the E-OBS daily precipitation and ERA5 daily maximum wind gusts. The ERA5 wind gust data has been interpolated onto a 0.25° grid to match the E-OBS data for the E-OBS/ERA5 dataset.

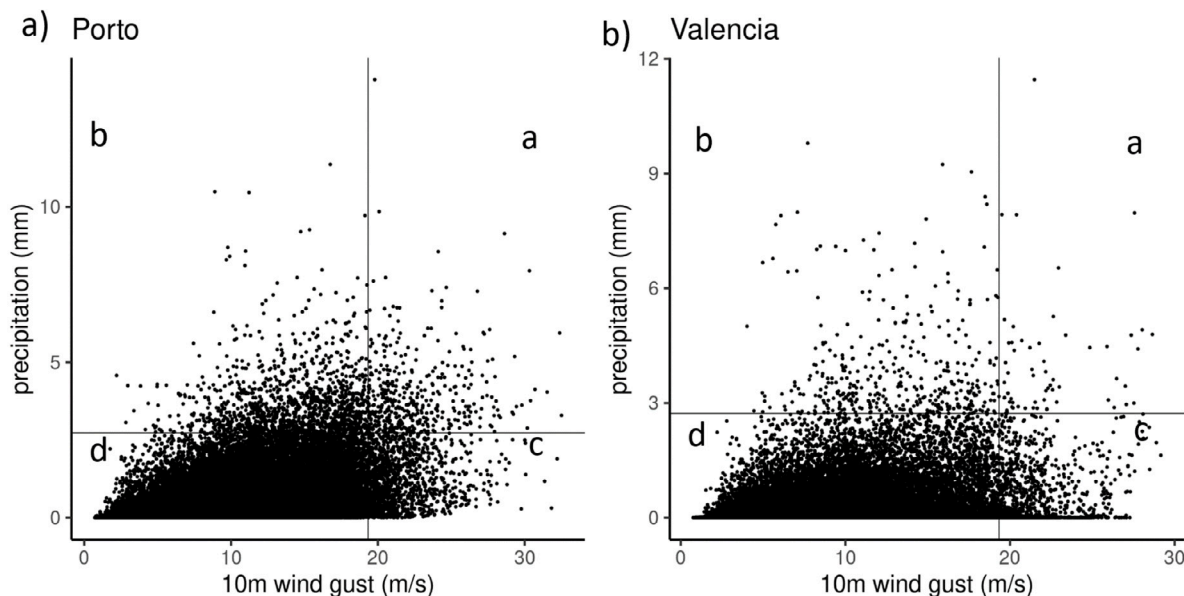


Fig. 1. Hourly 10 m wind gust and precipitation for (a) Porto and (b) Valencia, with horizontal and vertical lines at the 0.99 quantile for precipitation and wind respectively. a, b, c and d represent the four different quadrants of the graph. Quadrant a includes the extreme co-occurring, b extreme precipitation, c extreme wind and d non-extreme hourly events.

For the daily accumulations the ERA5 precipitation (or wind gusts) is the sum (or maximum) of the last 24 h of hourly precipitation (or wind gusts) from 00:00 to 23:00 each day. For the observational datasets the time interval for 24 h accumulated precipitation differs for each station and may comprise a 24 h period which included a portion of the previous day. All datasets in this study are from the period 1980 to 2018, for the winter half season, October to March. Both the ERA5 and E-OBS/ERA5 data considers a region from 20°W to 40°E and 30°S to 75°N. All GSOD and ECA stations used are also within this region.

## 2.2. Definition of extremes and their co-occurrence

For most of the analysis ERA5 precipitation and wind gusts above the 99th percentile for each gridpoint, for the winter half season, are taken as extreme (Pfahl and Wernli, 2012; Catto and Pfahl, 2013; Pfahl, 2014). When observational datasets are used, precipitation and wind gusts above the 80th percentile for each gridpoint and season are taken as extreme. A lower percentile is used in this case because many stations have incomplete timeseries for both precipitation and wind gust data and a higher percentile gives too small a sample size.

Wind gusts occur on short timescales, causing instantaneous damage. However precipitation characteristics are different depending on the timescale, since damage caused by precipitation depends on total run-off and is not instantaneous. For example lots of precipitation falling in an hour may cause an hourly extreme, and yet 24 h of light precipitation may cause a daily extreme. The hourly, 6 hourly, 24 hourly and 48 hourly precipitation accumulation extremes are studied here along with the maximum wind gust within these temporal periods. A co-occurrence is recorded if the precipitation accumulation and the maximum wind gust occur within the same time period, at the same gridpoint or station and are each above a particular percentile.

## 2.3. Extremal dependency

The conditional probability measure,  $\chi$ , was first introduced by Coles et al. (1999). It is the probability of one variable being extreme given that the other is extreme. At each gridbox

$$\chi(p) = Pr(Y(t) > y_p | X(t) > x_p) \quad (1)$$

where  $Y$  is precipitation,  $X$  is wind gust and  $y_p$  and  $x_p$  are the  $p$ th quantiles of  $Y$  and  $X$  with threshold probability  $p \in [0, 1]$ . In this case  $\chi$  is the probability of a precipitation (or wind) extreme occurring given a wind (or precipitation) extreme. Fig. 1 shows scatter plots of wind and precipitation for Porto (Portugal) and Valencia (Spain) with lines at the quantile 0.99. From Fig. 1  $\chi$  is estimated as

$$\chi = \frac{n_a}{n_a + n_b} = \frac{n_a}{n_a + n_c} = \frac{n_a}{(1-p)n} \quad (2)$$

where  $n$  is the total number of timesteps and  $n_a$ ,  $n_b$ ,  $n_c$  and  $n_d$  are the number of events in quadrants a, b, c and d respectively. All events have been included in our dataset including zero precipitation events. These event sets a, b, c and d will be referred to in the rest of this paper as the extreme co-occurring, extreme precipitation, extreme wind and non-extreme event sets respectively.

## 2.4. Time lag and lead analysis

To quantify the temporal separation between extreme wind and precipitation across Europe, an analysis allowing a maximum of 24 h lag and lead was performed. This gives insight into how  $\chi$  changes with hourly delays between the wind and precipitation extremes. Here

$$\chi(p, \tau) = Pr(Y(t + \tau) > y_p | X(t) > x_p) \quad (3)$$

where  $\tau$  is the number of hours that precipitation lags behind wind. The maximum  $\chi$  over  $\tau \in [-24, 24]$  and the lag or lead time that gives the maximum value of  $\chi$  at each gridbox are also calculated.

## 2.5. Extratropical cyclone identification and link to extreme events

Cyclones are identified and tracked using an objective feature-tracking algorithm to investigate events associated with cyclones (Hodges, 1994, 1995, 1999). The algorithm identifies vorticity maxima in the 6 hourly vorticity at 850 hPa. The vorticity data are truncated to T42 resolution before the tracking to focus on synoptic scale disturbances. A 6 hourly event is associated with a cyclone, and hence classed as a match, if said event occurs at the same 6 hourly timestamp and is within 1110 km (roughly 10°) from a cyclone track centre. The probability of a cyclone given an event is calculated by the following equation

$$Pr(\text{cyclone} | \text{event}) = \frac{100 \times M}{T} \quad (4)$$

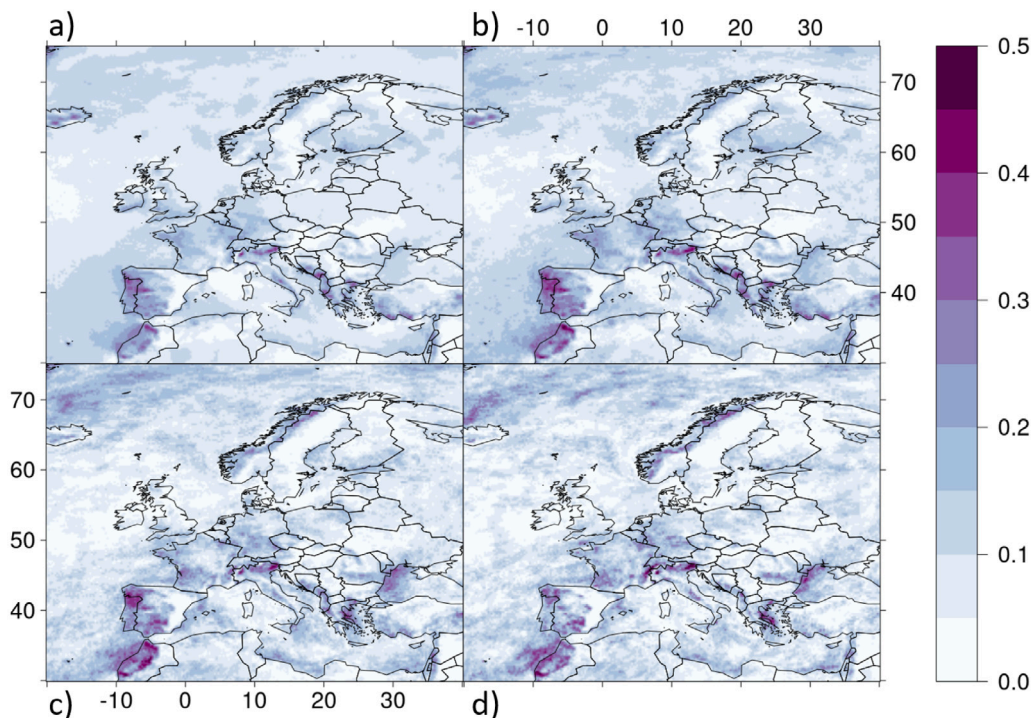


Fig. 2. Extremal dependency,  $\chi$ , maps for the 99th percentile extremes for the temporal accumulation periods (a) 1 h, (b) 6 h, (c) 24 h and (d) 48 h from the ERA5 dataset. The temporal periods are made using the summation of the last  $x$  number of hours of precipitation and the maximum wind gust within those hours.

where  $M$  is the number of matching events for a given gridpoint and  $T$  is the total number of events for a given gridpoint where  $T$  is equal to  $n_a$ ,  $n_b$ ,  $n_c$  or  $n_d$  depending on the event set. This was calculated for all four event sets, extreme co-occurring (a), extreme precipitation (b), extreme wind (c) and non-extreme (d). Due to the spherical nature of the Earth, to find the matching between events and cyclones, the spherical coordinates: Earth's radius, longitude and latitude ( $r$ ,  $\theta$ ,  $\varphi$ ) are transformed into the 3D Cartesian coordinates ( $x$ ,  $y$ ,  $z$ ), by the following equations

$$\begin{aligned} x &= r \sin \theta \cos \varphi \\ y &= r \sin \theta \sin \varphi \\ z &= r \cos \theta \end{aligned} \quad (5)$$

where  $r$  is the average radius of Earth, 6371 km,  $\theta \in (-\pi, \pi]$  and  $\varphi \in (-2\pi, 2\pi]$ . The following equation is used to find whether a cyclone track is nearby to a given gridpoint,

$$(x_T - x_E)^2 + (y_T - y_E)^2 + (z_T - z_E)^2 \leq 1110^2 \quad (6)$$

where  $x_T$ ,  $y_T$  and  $z_T$  are the cartesian coordinates for the cyclone track and  $x_E$ ,  $y_E$  and  $z_E$  are the cartesian coordinates for the ERA5 gridpoint. In this study  $1^\circ$  is taken to equal to 111 km, hence a cyclone is nearby a gridpoint if it is within 1110 km, because previous studies have used  $10^\circ$  spherical caps (Hawcroft et al., 2012).

### 3. Results

#### 3.1. ERA5 extremal dependency

The largest co-occurrences for Europe are around the western coasts of Portugal, Spain, France, the UK, and Norway, as well as the north eastern coast of the Mediterranean and regions south of the Alps (Fig. 2). The smallest co-occurrences are on eastern coasts of the UK, Sweden and Spain, over the north western coast of the Mediterranean and around the Carpathian and south eastern Norwegian mountain ranges. These results are consistent between accumulation periods and

generally agree with Martius et al. (2016); any disparities are discussed later in Section 4.

It has been suggested that the reason for low co-occurrence over east Norway and east Spain is the orographic enhancement of rain on the windward side of a mountain and the drying of the air by the time it reaches the lee (Martius et al., 2016). This means that while extreme winds extend eastward the extreme precipitation is only on the windward side of the mountain, this is seen in storm case studies (Martius et al., 2016). This could also explain the strong variations over France and the UK where the North Atlantic storm track sends cyclones moving approximately perpendicular to mountains or coasts. It could also explain the high co-occurrences over the eastern coasts of the Mediterranean, where cyclones from the Mediterranean storm track may arrive perpendicularly to the mountains on the western coast of Italy and the eastern coasts of the Adriatic Sea. It has also been suggested that the Cierzo winds may cause the low co-occurrence to the South of the Pyrenees (Martius et al., 2016). These winds affect the Ebro valley from Zaragoza to Barcelona during the winter half year (Tout and Kemp, 1985), although this does not explain the low co-occurrence over all of eastern Spain. Another reason that some places experience low co-occurrence could be seasonality. For example if an area experiences most of its extreme wind in one month and its extreme precipitation in another, the winter half year co-occurrence would be low. However a gridpoint analysis into regions with low co-occurrence was performed and seasonality did not occur (not shown). Composite plots shown later (Figs. 10–12) help to explain these differences in  $\chi$  in more depth along with their association to cyclones.

Over all temporal accumulation periods the spatial patterns of the hourly, 6 hourly, daily and 48 hourly  $\chi$  values are similar for regions of very large and very small  $\chi$  (Fig. 2). There are, however, more regions with very low  $\chi$  (less than 0.1) at longer temporal periods, suggesting that hourly and 6 hourly extremes co-occur more often than daily and 48 hourly extremes. This suggests cyclones moving through regions on a hourly timescale may be well associated with these extremes and are the main cause of co-occurrence.

The 6 hourly  $\chi$  values are up to 20% larger than the hourly for most regions in Europe (Fig. 3a). In contrast, for most of the UK,

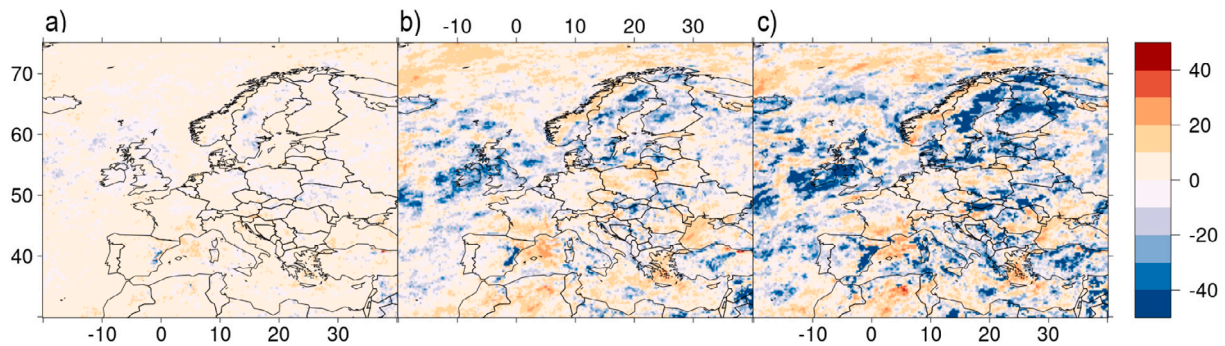


**Fig. 3.** Percentage difference,  $(\text{accumulated} - \text{hourly}) / ((\text{accumulated} + \text{hourly}) / 2) \times 100$ , between hourly and (a) 6, (b) 24 and (c) 48 hourly  $\chi$  values. Areas of red represent where the accumulated periods give higher  $\chi$  values and areas of blue represent where the hourly period gives higher  $\chi$  values. (For interpretation of the references to colour in this figure legend, the reader is referred to the web version of this article.)

Sweden, the east coast of Spain and parts of eastern Europe, hourly  $\chi$  is the largest and decreases by up to 50% with longer temporal periods (Figs. 3a, 3b and 3c). For Finland, Turkey, and the central Mediterranean decreases of 50% are also found with the 48 hourly accumulation, however 6 hourly  $\chi$  values in these regions are larger. This suggests that these countries have weather systems that move over quickly, dropping extreme precipitation within an hour or a few hours and have wind gust maxima that co-occur. Inspections of case studies (not shown) suggest that when precipitation is summed to daily or 48 hourly in these regions, precipitation is no longer extreme and hence no longer co-occurs with the wind gust extremes. It is also possible that these countries are affected by small weather systems where the extremes occur spatially close to each other and hence co-occur within a short timeframe.

Over Norway, the north west of the Black Sea, the north west of the Mediterranean, southern France, the east coast of Greece and parts of eastern Europe,  $\chi$  increases by up to 50% with longer accumulations (Figs. 3a, 3b and 3c). This suggests regions with higher co-occurrence at longer temporal precipitation accumulations have slow-moving weather systems, where precipitation falls consistently over a large number of hours or days, causing a daily or 48 hourly extreme. However when considering hourly timescales the precipitation would not be classed as extreme. These systems may also be large with large spatial gaps between the precipitation and wind gust extremes meaning that when considering hourly timescales co-occurrence is not found yet when daily or 48 hourly are considered co-occurrence is found.

### 3.2. Robustness of co-occurrence estimates using observational datasets

GSOD matches well with ERA5; both datasets have high co-occurrence over Portugal, the east of France and the west coasts of France and the UK (Figs. 4a and 4c). Low co-occurrence is found over southern France, the east of the UK and eastern Spain in both datasets too. However the GSOD dataset has less co-occurrence over Italy, the north east of the Mediterranean and Norway. The ECA data matches well with ERA5 too, both have high co-occurrence in northern Spain and western and central Germany (Figs. 4b and 4c). Low co-occurrence over eastern Spain is also found in both. The ECA dataset however also finds less co-occurrence over Norway. ERA5 gives larger values of  $\chi$  at each station than both the GSOD and ECA datasets (Figs. 5a and 5b). The correlation coefficients for the GSOD and ERA5 datasets and the ECA and ERA5 datasets are,  $r = 0.53$  and  $r = 0.59$  respectively. Hence ERA5 has a moderate positive correlation with both the GSOD and ECA datasets. To assess the joint tail distributions of the extremes we refer the reader to the two-dimensional extension of the skill score in Perkins-Kirkpatrick et al. (2007) introduced by Ridder et al. (2020).

The E-OBS/ERA5 dataset matches well with the ERA5 dataset in most regions for 80th percentile extremes with a correlation coefficient

**Table 1**

Mean (median) percentages of stations/gridpoints with matching in time extreme co-occurring daily events in ERA5 and station datasets over Europe. Higher percentages represent closer agreement in timings of co-occurring daily extreme events between the datasets.

	70th	80th	90th	99th
GSOD and ERA5	57% (61%)	47% (48%)	35% (29%)	3% (0%)
ECA and ERA5	67% (70%)	61% (65%)	53% (65%)	37% (16%)
E-OBS/ERA5 and ERA5	83% (84%)	79% (80%)	72% (73%)	56% (57%)

of  $r = 0.846$  (Figs. 6a, 6b and 5c). Both datasets also match well for 99th percentile extremes (not shown) with a correlation coefficient of  $r = 0.683$ . The ERA5 data again gives larger values of  $\chi$ , particularly over Norway, Iceland, Greece and Turkey, suggesting that ERA5 over estimates  $\chi$  over regions with high topography.

By comparing the dates for extreme co-occurring events in the ERA5 dataset with the three observational datasets, an analysis of how well the events match in time is performed (Table 1) for different extreme thresholds. For GSOD and ERA5, when looking at co-occurring events above the 70th percentile, the mean percentage of events over all stations that match in time is 57%. For larger extremes the mean percentage of matching events decreases significantly. Over half of the extreme co-occurring events in ECA and ERA5 datasets match in time for extremes above the 70th, 80th and 90th percentiles. For extreme events above the 99th percentile the mean percentage of matching events is 37%. Regions with low co-occurrence of extremes have poorly matching extreme co-occurring events for the higher percentiles due to little/no data. This is also true for stations with lots of missing data in our time series. Most of the extreme co-occurring events in the E-OBS/ERA5 dataset match events in ERA5, this is true even when looking at events above the 99th percentile. Overall, the ERA5 precipitation and wind gust extremes are occurring on the same days as the observational datasets most of the time, which means ERA5 is representing the timings of daily extreme co-occurring events well.

### 3.3. Non-simultaneous extremal dependency

The temporal separation between precipitation and wind extremes was relaxed to a maximum of 24 h to see how  $\chi$  changes with a delay between the wind and precipitation extremes. Previous studies have either made assumptions about the time lag and lead between precipitation and wind or have investigated it for a small number of cases (Raveh-Rubin and Wernli, 2015, 2016). Here the lag and lead is quantified for a larger number of events over the whole of Europe.

Over most regions  $\chi$  has no or little increase when including a 24 h lag and lead (Fig. 7a). Therefore most regions experience the largest  $\chi$  values when wind and precipitation extremes occur within the same hour. However in some regions  $\chi$  increases by up to 24%, although it is worth noting that most of these regions have relatively low  $\chi$  values

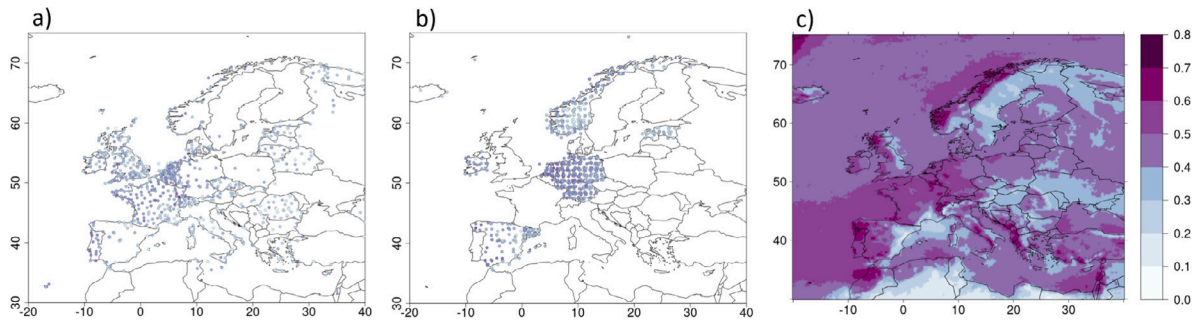


Fig. 4. Extremal dependency,  $\chi$ , maps for 80th percentile extremes from the (a) GSOD, (b) ECA, (c) ERA5 datasets.

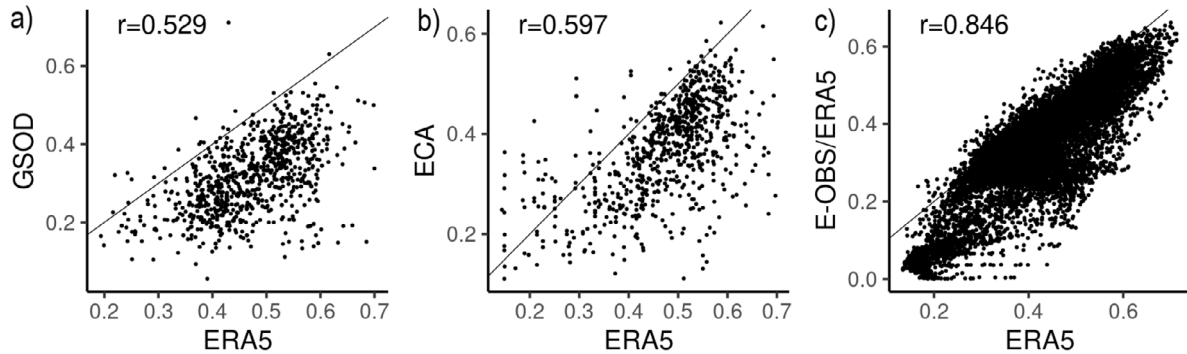


Fig. 5. Comparison between (a) GSOD and ERA5, (b) ECA and ERA5 to the nearest ERA5 grid box and (c) E-OBS/ERA5 and ERA5  $\chi$  values, with corresponding correlation coefficients,  $r = 0.529$ ,  $r = 0.597$ , and  $r = 0.846$ .  $\chi$  values of 0 (over the sea) from the E-OBS/ERA5 dataset have been removed.

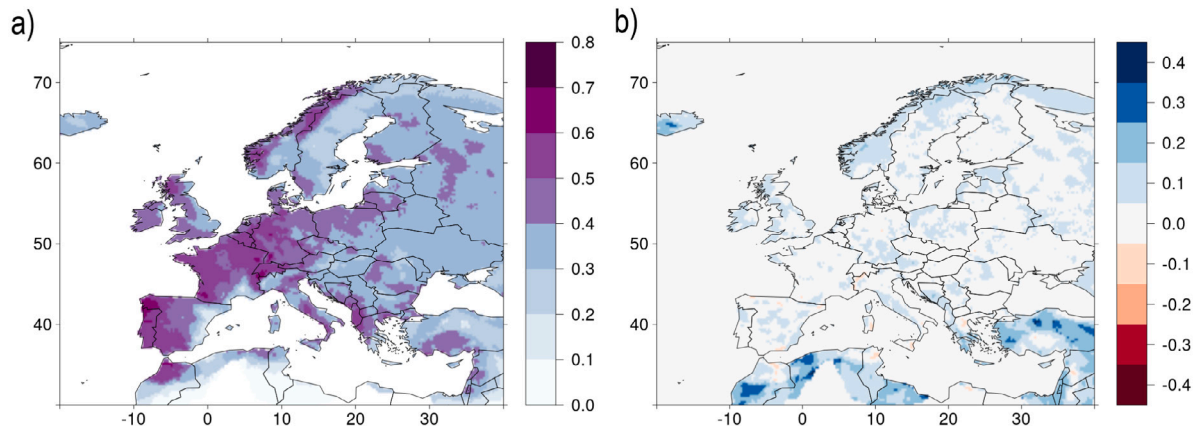


Fig. 6. (a) Extremal dependency,  $\chi$ , map for 80th percentile extremes from the ERA5/E-OBS dataset. (b) Difference in  $\chi$  between the ERA5/E-OBS and ERA5 datasets. A positive (blue) value indicates that the ERA5 dataset has a larger value of  $\chi$ . (For interpretation of the references to colour in this figure legend, the reader is referred to the web version of this article.)

even with this increase. The regions with the largest increases are Norway, Turkey, south east France and the Aegean sea. These regions are either on or surrounded by elevated topography (the Scandinavian Mountains, Pontic Mountains, Massif Central and Cretan Mountain ranges). Pfahl (2014) found that extreme precipitation events near elevated topography were further away from cyclone centres. Therefore elevated topography may be an explanation as to why a significant time lag occurs between the wind and precipitation extremes, if both these extremes are from the same weather system. Since the wind extremes may be nearer the centre of the cyclone, whereas the precipitation is further ahead or behind.

Most of the UK, France, Spain, Portugal, Belgium, the Netherlands, Finland, Italy and Germany experience the largest value of  $\chi$  when extreme wind and precipitation occur within the same hour (Fig. 7b).

As well as most of the North Atlantic, North and Norwegian Sea surrounding Europe. This would suggest that the same weather system is causing both extreme precipitation and wind gusts within these regions, this weather system would also be relatively small and/or fast moving. Or the extreme wind and rain are in similar regions spatially within the cyclone.

For south east France, Turkey and north eastern countries around the Mediterranean, largest  $\chi$  occurs when extreme wind gusts occur before precipitation extremes (Fig. 7b). This implies that storms causing these events are more likely to have extreme wind arriving before extreme precipitation. In a small region of south east France, wind gust extremes appearing between 8 and 12 h before precipitation extremes cause the largest  $\chi$  values. This is seen for Saint-Etienne in south east France which has a maximum  $\chi$  at 8 h (Fig. 8a). Over Turkey wind gust extremes appearing between 4 to 18 h before precipitation extremes

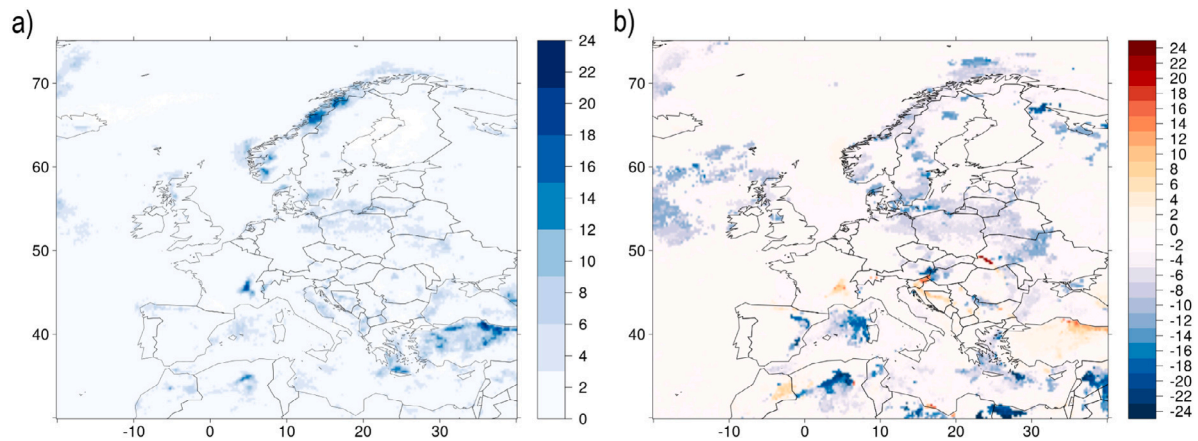


**Fig. 7.** (a) Percentage  $\chi$  increases when allowing up to a 24 h lag or lead between the precipitation and wind extremes for Europe. High percentages show regions where the highest  $\chi$  does not occur when extreme precipitation and wind occur within the same hour. (b) 24 h lag and lead times when  $\chi$  is at maximum. Red values indicate where wind gust extremes are arriving before precipitation extremes to give the largest  $\chi$ , white values where both extreme wind and precipitation arrive within the same hour to give the largest  $\chi$  and blue values where precipitation extremes are arriving before wind gust extremes to give the largest  $\chi$ . (For interpretation of the references to colour in this figure legend, the reader is referred to the web version of this article.)

cause the largest  $\chi$  values. The larger of these lags occur over the north coast, as seen for Samsun in north Turkey which has a maximum  $\chi$  at 12 h (Fig. 8b). Over countries to the north east of the Mediterranean, wind gust extremes arriving between 2 to 14 h before precipitation extremes cause the largest values of  $\chi$ .

For Norway, south Sweden, north west Scotland, the Aegean sea, east Germany, Poland, Ukraine, Belarus, Lithuania, the north west of the Mediterranean and the east coast of Spain the largest  $\chi$  occurs when precipitation extremes occur before wind gust extremes, within the range of 6 to 24 h (Fig. 7b). This implies that storms causing these events are more likely to have extreme precipitation arriving 6 to 24 h before extreme wind. This is seen for Fort William in north west Scotland which has maximum  $\chi$  at  $-7$  h, when precipitation arrives 7 h before wind (Fig. 8c). And Gdynia in north Poland has maximum  $\chi$  at  $-14$  h, with a second peak at  $-5$  and  $-7$  h (Fig. 8d). For the Mediterranean the largest  $\chi$  occurs when precipitation extremes occur between 2 to 24 h before the wind extremes, with large regions occurring between 12 to 16 h before. This is in agreement with Raveh-Rubin and Wernli (2015), where the precipitation peak typically occurred 12 h before the wind gust maximum. And Raveh-Rubin and Wernli (2016), where the precipitation peak occurred 6 h (or less) before the wind gust maximum.

For all the locations on Fig. 8 there are peaks in the  $\chi$  values with significant drops either side. This suggests that for certain locations there is a significant time separation between the wind and precipitation extremes. These lag and lead times vary between locations yet the maxima are well within 24 h, suggesting weather systems causing these extreme wind and precipitation events affect a region over hours rather than days.

### 3.4. Cyclones and extreme co-occurring events

The probability of the presence of a cyclone given an 6 hourly extreme co-occurring event is particularly high over the Mediterranean, the UK and northern Europe (Fig. 9a), with a mean probability over Europe of 81%. Few regions have lower percentages than 50%. These occur in a narrow band over southern Spain, southern France, northern Italy and along the continent to Romania. In these regions cyclones are associated with extreme co-occurring events less than half the time. Or they are further away than 1110 km from the co-occurring extremes location, for example, precipitation and wind extremes in the Iberian peninsula are associated with atmospheric rivers more than 48% of the time (Waliser and Guan, 2017). Atmospheric rivers are typically associated with a low-level jet stream ahead of the cold front of an

extratropical cyclone, far away from the cyclone centre. France and around the Alps also have high percentages of extreme precipitation associated with atmospheric rivers (24% to 48%), however wind extremes in these regions only have percentages of 12% to 36% (Waliser and Guan, 2017).

The spatial pattern for the probability of the presence of a cyclone given an 6 hourly extreme precipitation event (Fig. 9b) is similar to that of the extreme co-occurring events, with a slightly lower probability of occurring with a cyclone, with a mean probability over Europe of 73%. The spatial pattern for extreme wind events (Fig. 9c) is again similar to that of the co-occurring and also has similar percentages, with a mean probability over the region of 81%. Non extreme events (Fig. 9d) have the smallest percentages, with a mean probability over the region of 49%, again with similar spatial patterns to the other event sets.

For Porto, Portugal, almost all nearby cyclones linked to extreme co-occurring, extreme precipitation and extreme wind events are over the North Atlantic, north and west of the gridpoint (Figs. 10a, 11a and 12a). Hence Porto may have a large  $\chi$  value because the same weather systems cause both the precipitation and wind extremes. For the co-occurring events, the minimum in mean sea level pressure (MSLP) is to the north west, indicating that the co-occurring extremes occur in the cold frontal region of storms yet further away than 1110 km. This may be why the percentage of extreme co-occurring events associated with cyclones in this region is only 56% (Fig. 9a).

For Bergen, Norway, most extreme co-occurring, extreme precipitation and extreme wind events nearby cyclones are to the west and north west over the North Atlantic (Figs. 10c, 11c and 12c). However extreme wind event cyclones are also directly over Bergen and to the east. Again, this suggests why  $\chi$  is large over this region, yet not as large as Porto. The minimum in MSLP for the co-occurring extremes is to the north west, nearby Bergen.

For Valencia, East Spain, nearby cyclones linked to extreme co-occurring events are mostly to the south, over southern Spain and Portugal, over the western Mediterranean and over north Africa, similarly with the cyclones linked to extreme precipitation events (Figs. 10b and 11b). The minimum in MSLP is almost directly over Valencia with a south east tilt for the co-occurring extremes and similarly for the precipitation extremes. Cyclones near the wind extremes are mostly to the east of Valencia over the Mediterranean with the minimum MSLP over the west of the Mediterranean (Fig. 12b). If wind extremes are mainly caused by cyclones over to the south of Valencia and precipitation extremes from cyclones over to the west this may be why Valencia and the eastern coast of Spain have few co-occurring events since the different extremes are caused by different weather systems.

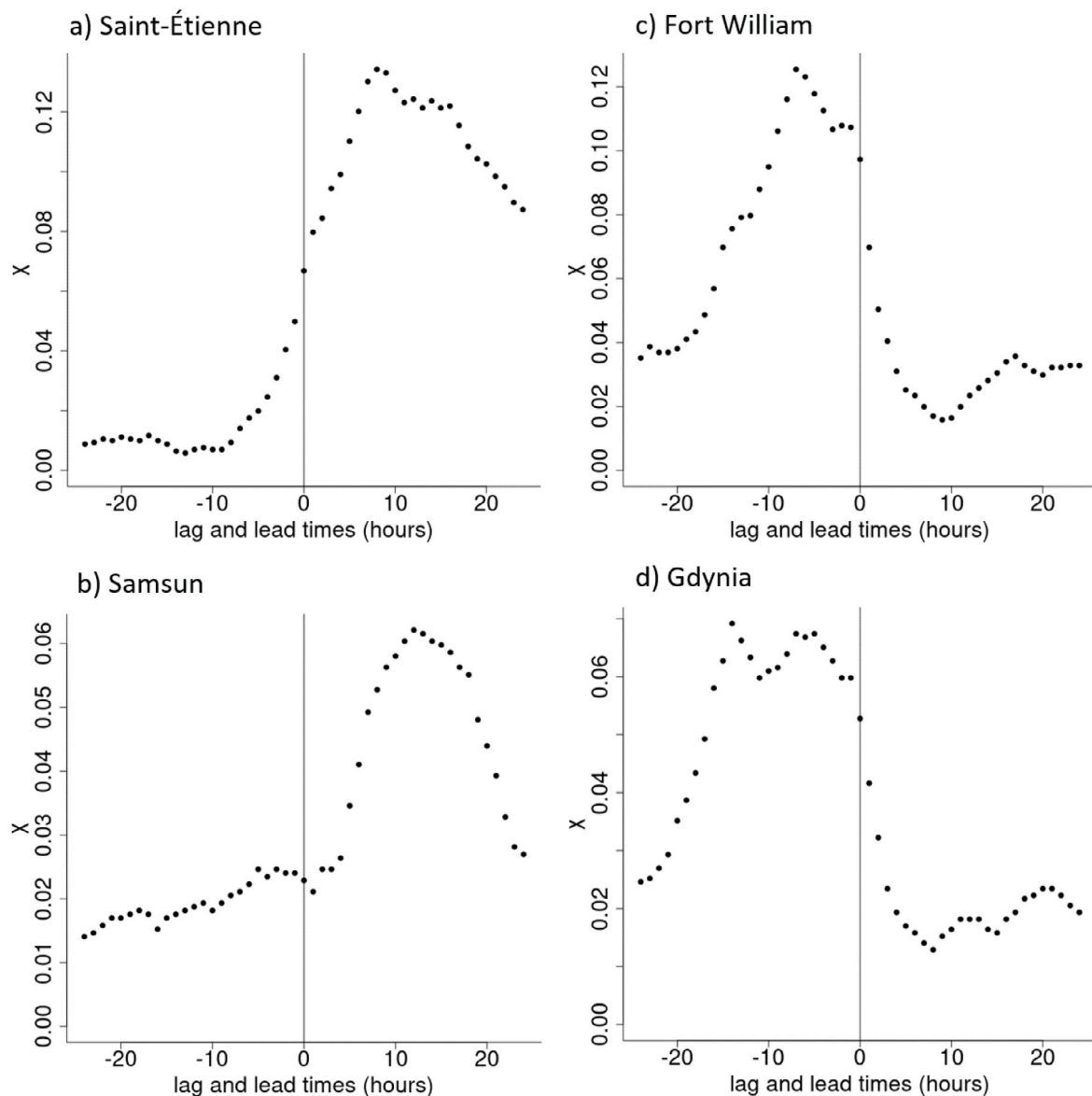


**Fig. 8.**  $\chi$  values for each 24 h lag and lead time for (a) Saint-Etienne, (b) Samsun, (c) Fort William and (d) Gdynia. Positive hours are when the largest  $\chi$  is given when the extreme wind gusts are occurring before the precipitation extremes and the negative hours are when the largest  $\chi$  is given when the precipitation extremes are occurring before the wind gust extremes.

The probability of a cyclone given a co-occurring extreme at Valencia is 63% (Fig. 9a), suggesting other weather systems may be causing the other 37% of extreme co-occurring events.

For Stockholm, Sweden, extreme co-occurring and extreme precipitation cyclones are located to the south and west, over the Baltic Sea, North Sea, Sweden and Norway (Figs. 10d and 11d). Cyclones linked to extreme wind are also in these regions but are more frequently to the north and east of Stockholm over the north Baltic Sea and Finland (Fig. 12d). Like Valencia, Stockholm also has a low co-occurrence of extreme events, which again may be because different weather systems cause the different extremes. Stockholm has a large probability, 87%, of a cyclone given a co-occurring extreme (Fig. 9a), this is perhaps surprising since we can see many cyclone tracks further away than 1110 km but related to the MSLP minimum to the north west of the gridpoint.

To the south of the Alps (northern Italy) large co-occurrence is found. For Treviso, northern Italy, cyclones linked to extreme co-occurring and extreme precipitation events are mostly located in a small cluster south west of the gridpoint over the north of the Mediterranean (Figs. 10e and 11e). Cyclones linked to extreme wind events

are also mainly in this region but with more of a spread over Italy and further south of the Mediterranean (Fig. 12e). This suggests why the south east of the Alps over Treviso has a large  $\chi$  value. For the extreme co-occurring events the minimum in MSLP is to the south west close to the gridpoint.

To the east of the Alps (Austria, Slovenia, Hungary) low co-occurrence is found. Therefore, Budapest has few cyclones nearby when co-occurring events occur (Fig. 10f). It does, however, have many cyclones nearby to extreme precipitation events (Fig. 11f). These cyclones occur in a large cluster to the south and south west over Italy and the northern Mediterranean, as well as further away and more spread out in the north. Cyclones linked to wind extremes are mainly to the north east of Budapest in a large cluster over eastern Europe, with a few nearby Budapest but to the south over the Mediterranean (Fig. 12f). The different weather systems causing these extremes would again suggest why Budapest has such a low co-occurrence, agreeing with Martius et al. (2016) and Pfahl (2014).

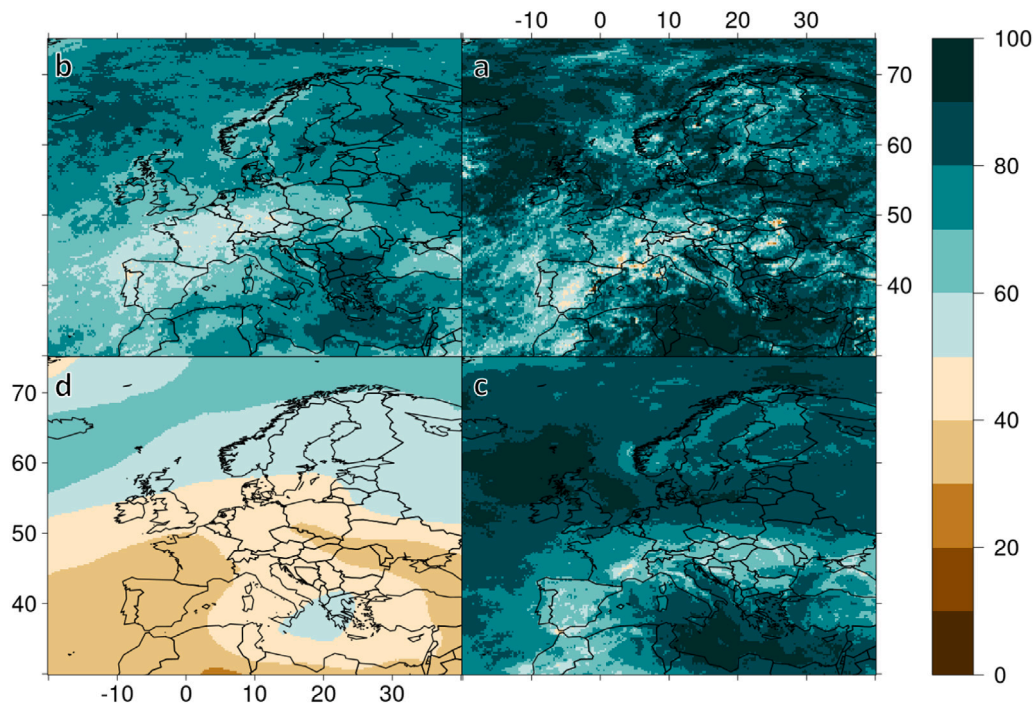


**Fig. 9.** Estimates of the probability of the presence of a cyclone given the 6 hourly event sets a, b, c and d. Where a are the percentages of extreme co-occurring, b extreme rain, c extreme wind and d non-extreme 6 hourly events. A cyclone is counted for a gridpoint if the gridpoints event occurs at the same 6 hourly timestamp and is within 1110 km from the cyclone tracks centre.

Large co-occurrence is also found along the east coast of the Mediterranean. Over Podgorica, Montenegro, nearby cyclones to extreme co-occurring and extreme precipitation events are mainly clustered to the west over Italy, the Adriatic Sea and the Tyrrhenian Sea (not shown). Wind extremes are in similar regions with some shifted east, agreeing with Pfahl (2014), where precipitation and wind extremes for south eastern Europe were linked to cyclones over these same regions. Again this suggests that the reason for high co-occurrence is because the same weather systems cause both extremes. For the extreme co-occurrence events the minimum in MSLP is to the north west close to gridpoint.

#### 3.4.1. Cyclone characteristics

We have shown that cyclones are important for co-occurring extremes, but a question remains as to whether these cyclones have particular characteristics.

For all event sets the most intense cyclones occur over the North Atlantic storm track (Fig. 13). The mean vorticity of cyclones for the extreme co-occurring events is larger than that for the non-extreme events for all of Europe (Fig. 14c). Similarly extreme precipitation events have a smaller cyclone vorticity than the co-occurring for most regions, excluding a few regions around the north and north east coast of the Mediterranean (Fig. 14a). However the extreme precipitation events cyclones have a larger intensity than the non-extreme events (Fig. 13). This agrees with Pfahl and Wernli (2012) where cyclone intensity was higher for cyclones associated with extreme precipitation along Europe's western coasts. The percentage change between extreme co-occurring events and extreme wind events mean vorticity decreases for some places in Europe (Fig. 14b). Hence cyclones near extreme wind and extreme co-occurring events have mean vorticity larger than the other two event sets for Europe.

For all event sets the fastest cyclones occur over the North Atlantic, the UK, Northern and Central Europe (Fig. 15). The slowest cyclones occur over the Mediterranean. These spatial patterns and magnitudes agree well with Hoskins and Hodges (2002). The mean speed of cyclones for the extreme co-occurring events is faster than

extreme precipitation events for most of the North Atlantic, the UK, Central and much of Northern Europe (Fig. 16a). The mean speed of cyclones for the extreme co-occurring events is slower than wind extreme events for much of Europe, particularly over the east of Spain, the Mediterranean and Sweden (Fig. 16b). The mean speed of cyclones for the extreme co-occurring events is faster than non extreme events for most of Europe (Fig. 16c). The mean speed of cyclones for the extreme co-occurring events is slower over much of the Mediterranean for all datasets. This may suggest that fast cyclones cause extreme co-occurring 6 hourly events over Europe yet slow cyclones cause extreme co-occurring 6 hourly events over the Mediterranean.

## 4. Summary and discussion

This study has identified extreme precipitation and extreme wind events in the ERA5 reanalysis dataset using a definition of extremes of the 99th percentile. The frequency of these co-occurring extremes have been quantified over Europe for different timescales and in relation to extratropical cyclones. The main conclusions are given below in reference to the questions posed in the introduction, along with the main discussion points.

1. What is the spatial distribution of the probability of co-occurrence of extreme precipitation and extreme winds over Europe in the reanalysis and observational datasets?

For the winter half year, Europe's western coasts, the north eastern coast of the Mediterranean and south of the Alps experience the highest values of co-occurrence of extreme precipitation and wind. Eastern coasts, the north western coast of the Mediterranean and around the Carpathian and the south eastern Norwegian mountain ranges experience the lowest values of co-occurrence.

Comparing results with Martius et al. (2016), 24 h  $\chi$  for January to February 98th percentile extremes (supporting information from Martius et al. (2016)), similar values and spatial patterns of  $\chi$  are found. The magnitudes in our study are lower around the

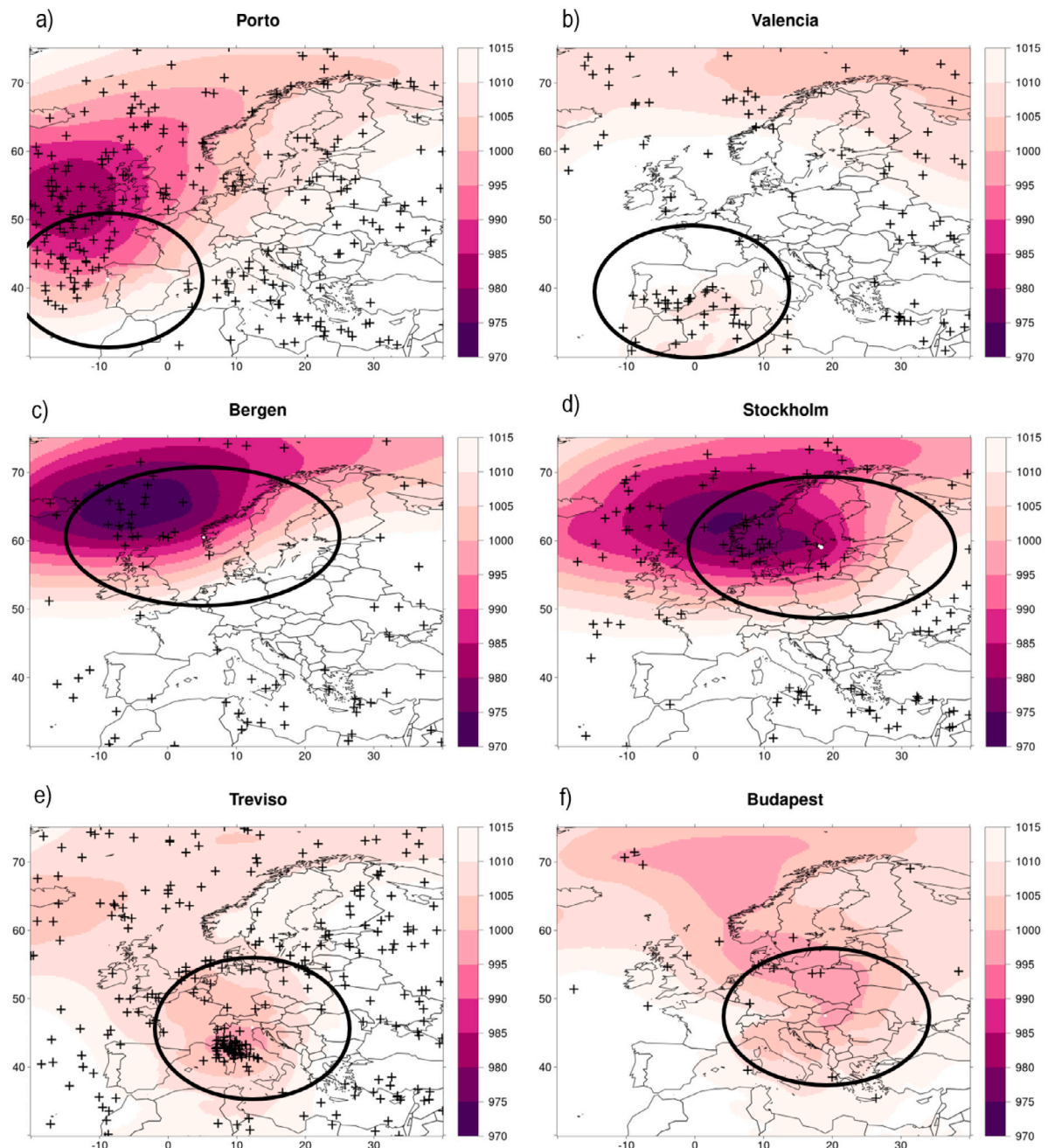


**Fig. 10.** Average MSLP plots for the extreme co-occurring events at locations (a) Porto, (b) Valencia, (c) Bergen, (d) Stockholm, (e) Treviso and (f) Budapest. These locations are selected due to their very low or very high  $\chi$  values. Crosses are the positions of cyclones identified by TRACK at the time of the extreme co-occurring events. Black circles indicate the approximate search regions.

Carpathian mountain ranges and over the North and Baltic Seas, and higher over North Italy. These differences may be associated with the choice of the definition of extremes, the season and the spatial relaxation in matching criteria. Where the values in our study are higher, this could be associated with the higher spatial resolution of ERA5, which may represent features over high orography better than ERA-Interim.

For most regions of Europe, the observational datasets have the same spatial pattern of 80th percentile co-occurrence as ERA5. However the observational datasets have lower  $\chi$  values. This may be because the ERA5 data is averaged over a 31 km gridbox whereas the observational station data is from a gridpoint. Hence a larger area is allowed for a match between the extreme wind and precipitation within the ERA5 data so larger  $\chi$  values are

found. Particularly higher values in ERA5 are also found over topography. Overall we can be confident in our results of spatial co-occurrence over most of Europe but should be wary that our values of  $\chi$  may be too high for individual locations, particularly over high topography. However in terms of impact, understanding co-occurrence at larger spatial areas is more useful than at individual stations.

The mean percentage of extreme events that match in time between ERA5 and the observational datasets is high (more than 50% matching). This means that ERA5 precipitation and wind gust extremes are occurring on the same days as the observational datasets most of the time, and ERA5 is representing the timings of daily extreme co-occurring events well. The differences in these timings may come from differences in

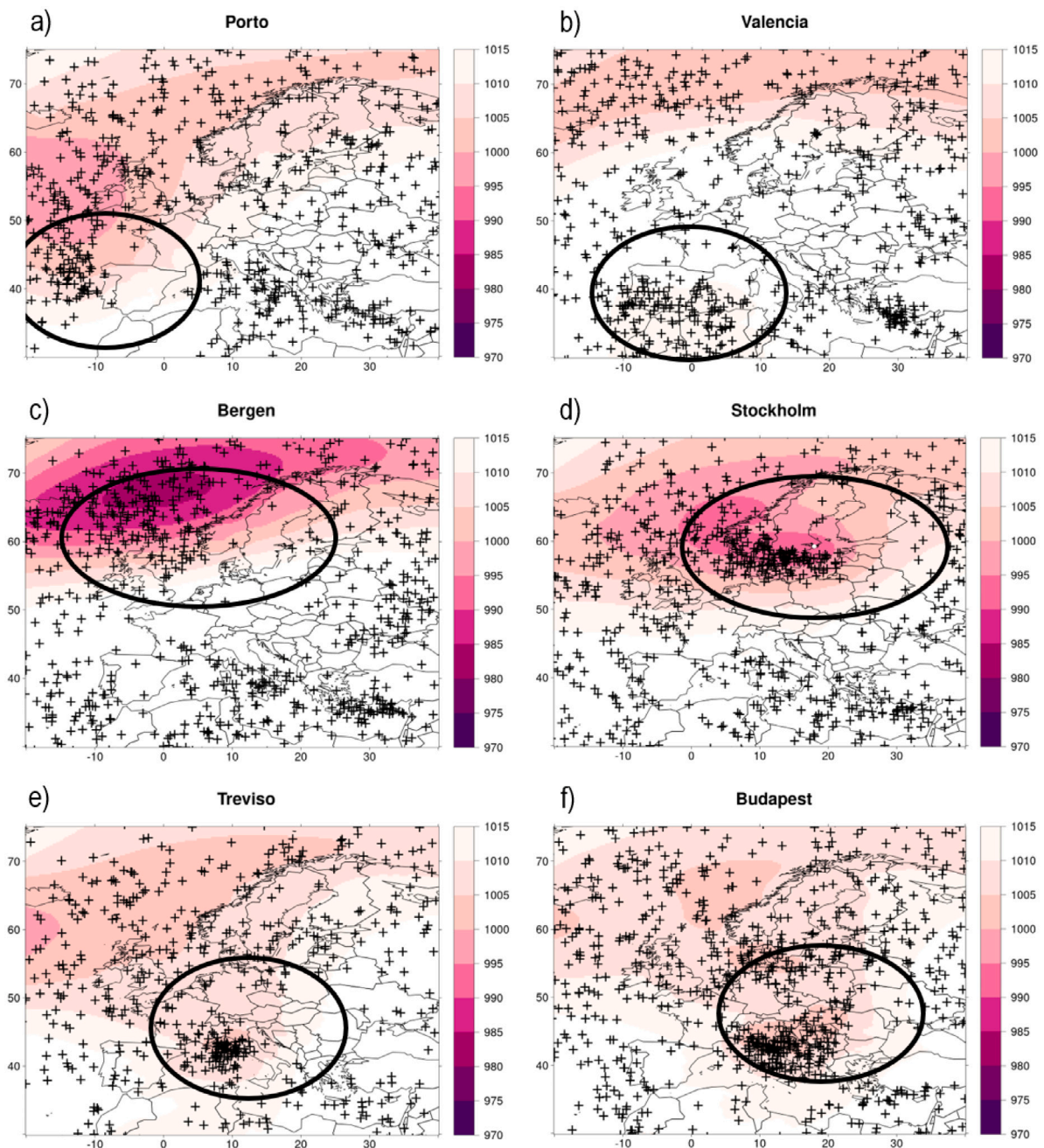


Fig. 11. As Fig. 10 but for the extreme precipitation events.

the timings of precipitation accumulation between ERA5 and the station datasets. ERA5 daily precipitation accumulation is from midnight each day, however the observational datasets precipitation accumulations vary per station and may make up a 24 h period which included the previous day.

Additionally there are other problems with trying to compare ERA5 to observational datasets. Firstly, only daily comparisons can be made meaning we have no way of investigating the robustness in our hourly ERA5 data. Secondly, the observational station data has many missing days in our timeseries due to missing data. This along with regions of low co-occurrence means some regions have very few events to look at.

## 2. How does the temporal scale of the precipitation extremes affect the co-occurrence?

Over all temporal precipitation accumulation periods, regions of very high or very low co-occurrence are consistent. There are however more regions with very low co-occurrence at higher

accumulations. Over the UK, Eastern Spain, Sweden and Finland co-occurrence decreases by up to 50% with longer accumulations. Over Norway, the north west of the Black Sea, the north west of the Mediterranean, southern France, the east coast of Greece and parts of eastern Europe, co-occurrence increases by up to 50% with longer accumulations.

## 3. Can we quantify the temporal offset of the extreme precipitation and winds over Europe?

Extremal dependence in most regions has little increase by including a  $\pm 24$  h delay between precipitation and wind. This would suggest that the same weather systems are causing both extreme precipitation and wind gusts within these regions. However for certain regions there is a significant time separation between the wind and precipitation extremes.  $\chi$  increases by up to 24% are over regions either on or surrounded by elevated topography, agreeing with Pfahl (2014) that precipitation extreme

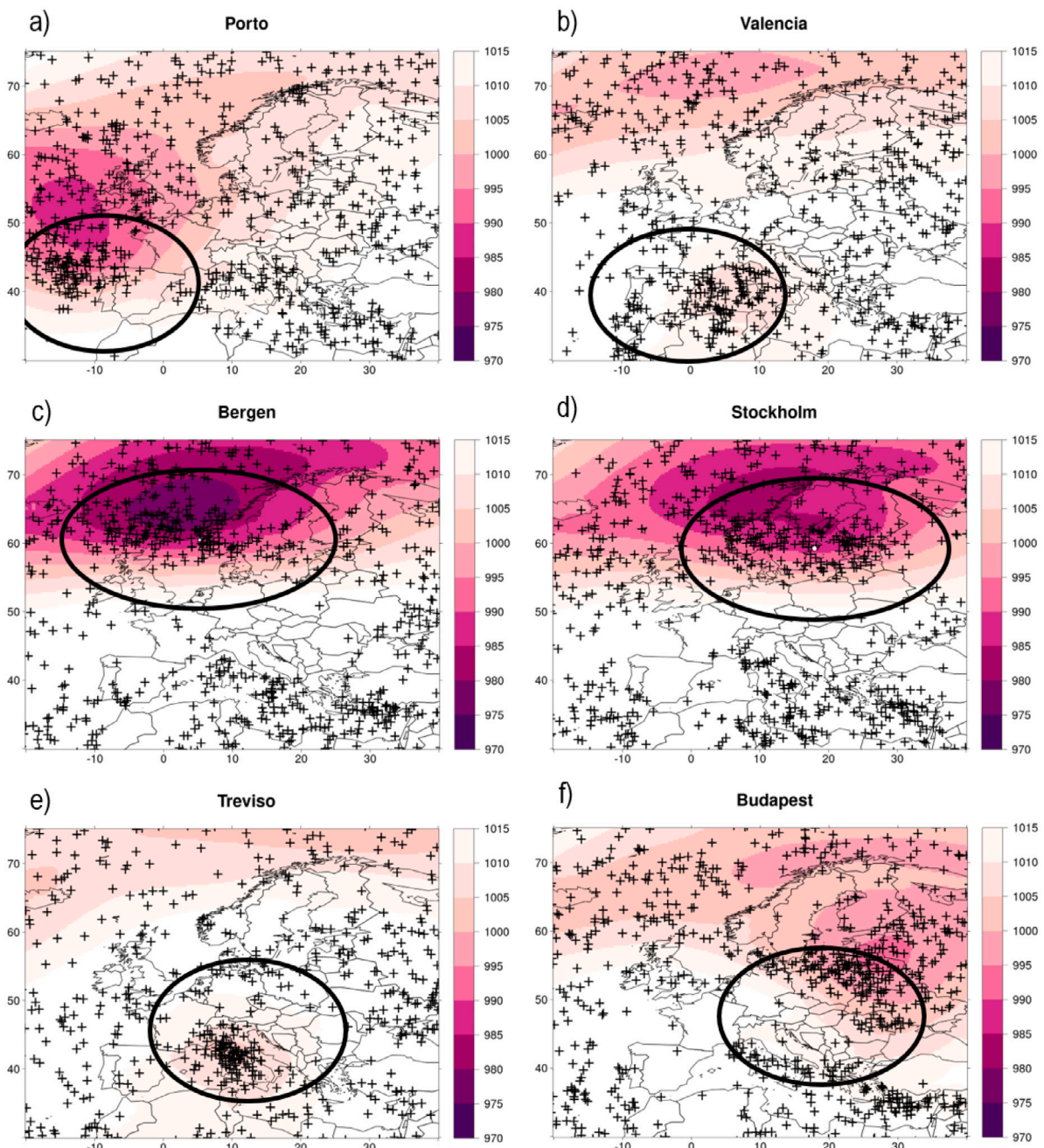


Fig. 12. As Fig. 10 but for the extreme wind events.

events near elevated topography are further away from cyclone centres.

4. How strongly related are the co-occurrence of extremes to extratropical cyclones and are there preferred cyclone characteristics? For all of Europe extreme co-occurring events are associated with cyclones far more of the time than non-extreme precipitation and wind events. For most of Europe, given an extreme co-occurring event, cyclones occur nearby more than 70% the time. The largest percentages occur in the North Atlantic and Mediterranean storm track regions. However a narrow band over southern Spain, southern France, northern Italy and along the continent to Romania has much lower percentages, of less than 50%. Precipitation and wind extremes in these regions are heavily associated with atmospheric rivers (Waliser and Guan, 2017), and composite plots of MSLP show that co-occurring extremes occur in the cold frontal regions of storms yet further

away than 1110 km. These plots also indicate that regions with small  $\chi$  have extremes caused by different weather systems and that regions with large  $\chi$  have both extremes caused by the same weather system.

Cyclones linked with extreme events, particularly extreme co-occurring and extreme wind, have the largest vorticity, indicating that these systems are near their time of maximum intensity. The mean speed of cyclones are faster for extreme co-occurring events and extreme wind events over most of Europe. The Mediterranean is an exception, where extreme events have slower cyclones.

Within extratropical cyclones there are a number of locations that tend to have high wind speeds, such as the warm conveyor belt, the cold conveyor belt, and the sting jet (close to the centre of the cyclone; (Hewson and Neu, 2015)). The location of the heaviest precipitation within extratropical cyclones is typically in the warm frontal

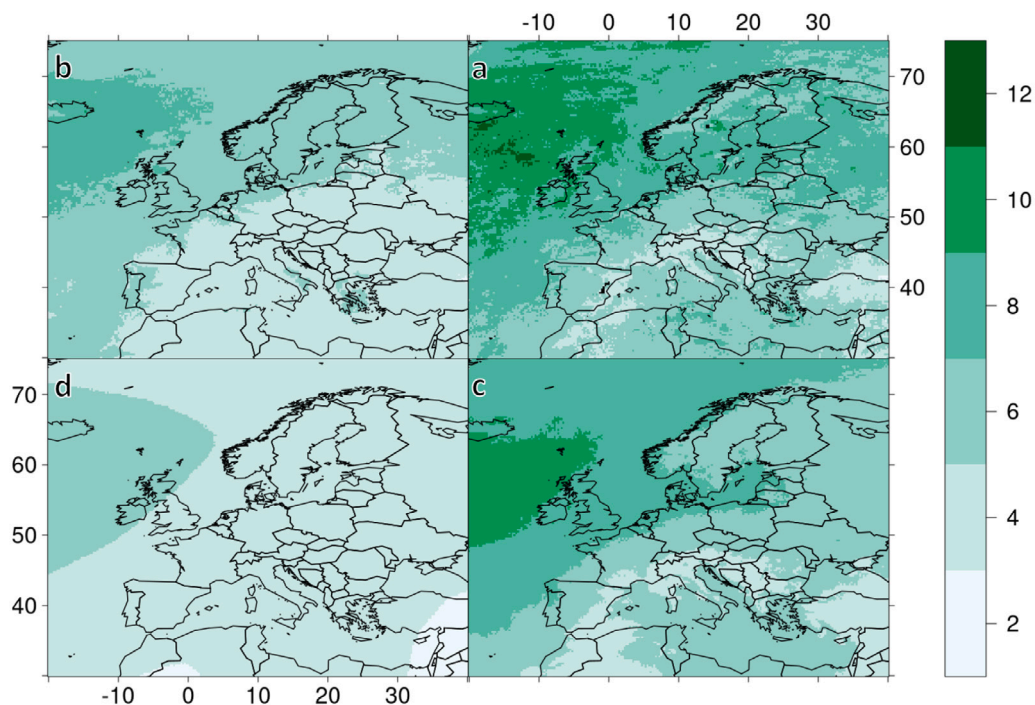


Fig. 13. The mean vorticity (rad/s) of cyclones given the 6 hourly event sets a, b, c and d. Where a are the extreme co-occurring, b extreme precipitation, c extreme wind and d non-extreme 6 hourly events. These panels indicate the relative difference in intensity to the local average intensity.

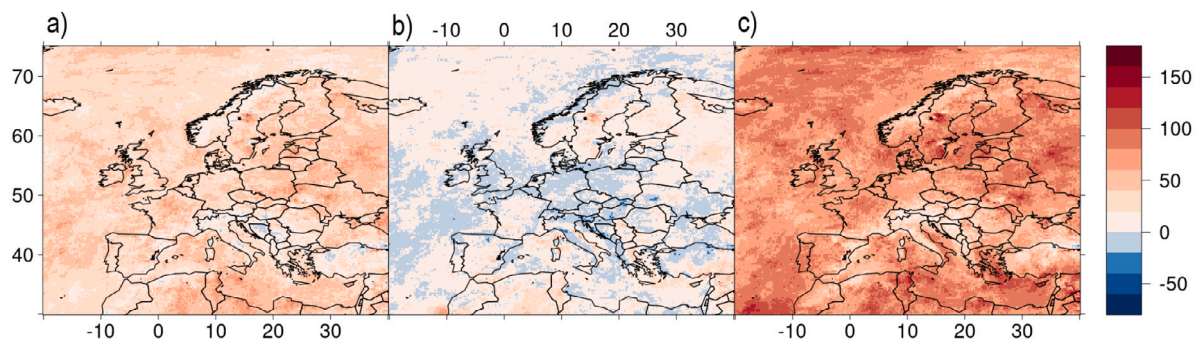


Fig. 14. The percentage change,  $((\zeta_a - \zeta_b)/\zeta_b) \times 100$ , between event set a's mean vorticity ( $\zeta_a$ ) of a cyclone and (a) b ( $\zeta_b$ ), (b) c ( $\zeta_c$ ) and (c) d ( $\zeta_d$ ).

region and along the cold front, as seen in case studies and composites (Browning, 1986; Catto and Pfahl, 2013; Hawcroft et al., 2017). The outcomes of the precipitation accumulation and temporal separation analysis performed here point to regional differences in the particular sectors of the cyclones that cause the extremes at different timescales. For example, when the co-occurrence is higher for shorter accumulations, this could be associated with intense short-duration rainfall along cold fronts (Browning, 1986) coinciding with strong winds in the warm conveyor belt region (Hewson and Neu, 2015).

A Lagrangian (cyclone centric) perspective is needed to look at the spatial structure of extremes within extratropical cyclones, and the relationship between the speed and intensity of cyclones in more detail. Other characteristics such as direction, size and lifecycle could also be important for determining which cyclones cause these co-occurring extremes.

#### CRedit authorship contribution statement

**Laura E. Owen:** Conceptualization, Methodology, Software, Validation, Formal analysis, Investigation, Data curation, Writing - original draft, Visualization. **Jennifer L. Catto:** Conceptualization, Writing - review & editing, Supervision. **David B. Stephenson:** Conceptualization, Writing - review & editing, Supervision. **Nick J. Dunstone:** Conceptualization, Supervision.

#### Declaration of competing interest

The authors declare that they have no known competing financial interests or personal relationships that could have appeared to influence the work reported in this paper.

#### Acknowledgements

We acknowledge the data providers in the ECA&D project. Klein Tank, A.M.G. and Coauthors, 2002. Daily dataset of 20th-century surface air temperature and precipitation series for the European Climate Assessment. *Int. J. of Climatol.*, 22, 1441–1453. Data and metadata available at <https://www.ecad.eu>.

We acknowledge the E-OBS dataset and the data providers in the ECA&D project (<https://www.ecad.eu>). Cornes, R., G. van der Schrier, E.J.M. van den Besselaar, and P.D. Jones. 2018: An Ensemble Version of the E-OBS Temperature and Precipitation Datasets, *J. Geophys. Res. Atmos.*, 123. doi:10.1029/2017JD028200.

D.B. Stephenson thanks O. Martius for clarification concerning how conditional probabilities were calculated in Martius et al. (2016).

L.E. Owen is supported by the College of Engineering, Mathematics and Physical Sciences studentship, UK.

J.L. Catto was partly funded by the Natural Environment Research Council (NERC) STORMY-WEATHER grant (NE/V004166/1).

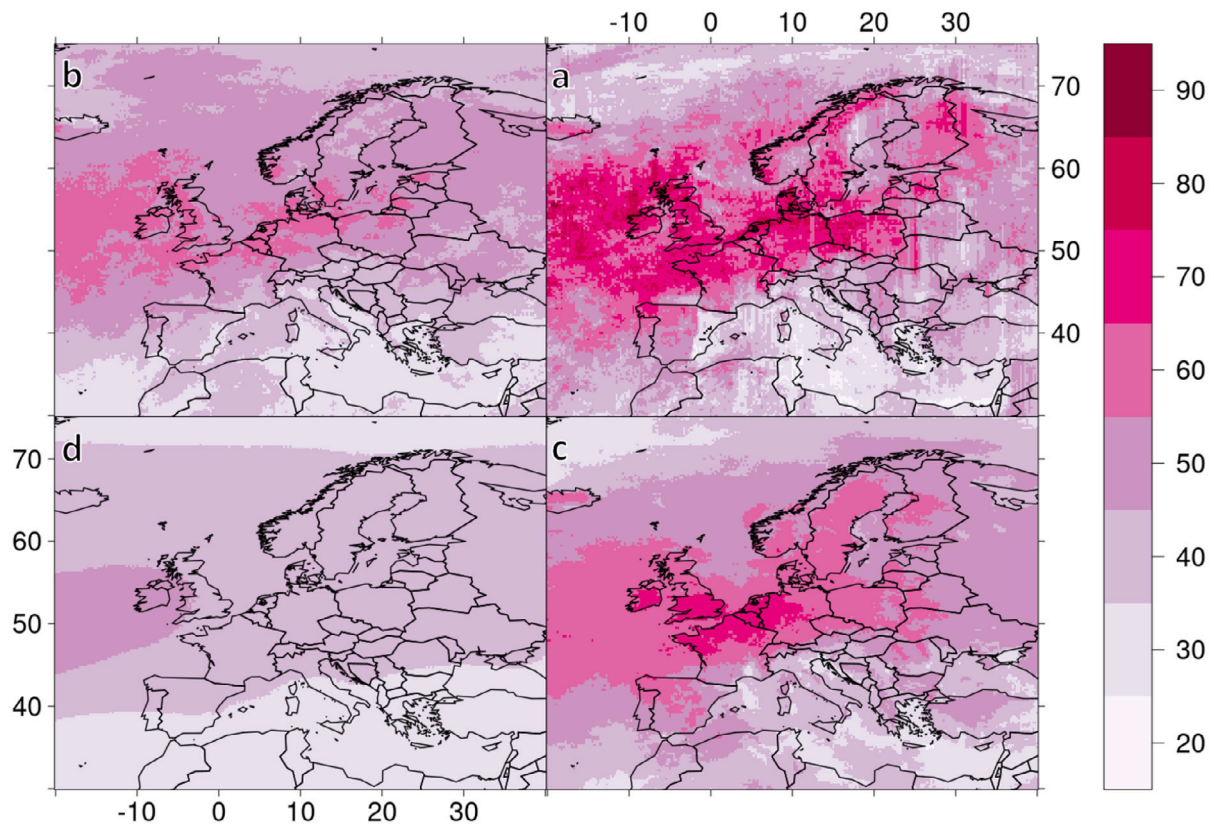


Fig. 15. The mean speed (km/h) of cyclones given the 6 hourly event sets a, b, c and d. Where a are the extreme co-occurring, b extreme precipitation, c extreme wind and d non-extreme 6 hourly events.

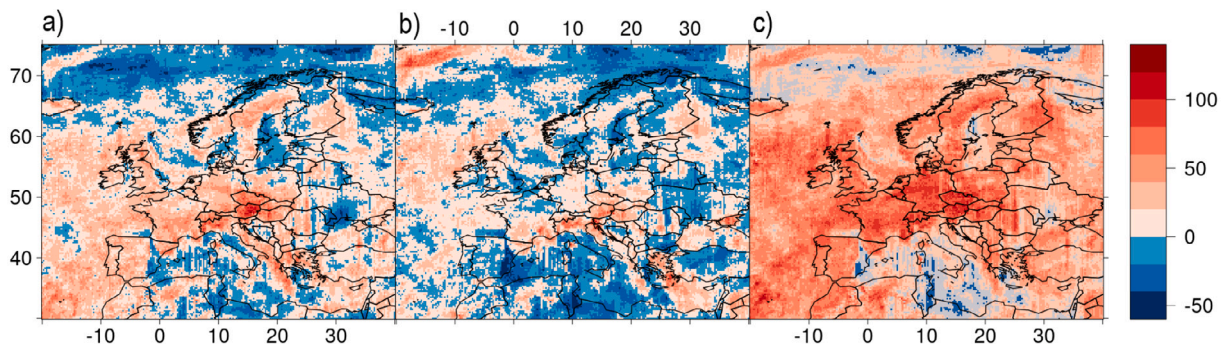


Fig. 16. The percentage change,  $((u_a - u_b)/u_b) \times 100$ , between event set a's mean speed ( $u_a$ ) of a cyclone and (a) b ( $u_b$ ), (b) c ( $u_c$ ) and (c) d ( $u_d$ ).

N.J. Dunstone was supported by the Met Office Hadley Centre Climate Programme funded by BEIS and Defra.

## References

- Barbero, R., Fowler, H.J., Blenkinsop, S., Westra, S., Moron, V., Lewis, E., Chan, S., Lenderink, G., Kendon, E., Guerreiro, S., Li, X.-F., Villalobos, R., Ali, H., Mishra, V., 2019. A synthesis of hourly and daily precipitation extremes in different climatic regions. *Weather Clim. Extrem.* 26, 100219.
- Browning, K.A., 1986. Conceptual models of precipitation systems. *Weather Forecast.* 1 (1), 23–41.
- Catto, J.L., Pfahl, S., 2013. The importance of fronts for extreme precipitation. *J. Geophys. Res.: Atmos.* 118 (19), 10,791–10,801.
- Coles, S., Heffernan, J., Tawn, J., 1999. Dependence measures for extreme value analyses. *Extremes* 2, 339–365.
- Cornes, R.C., van der Schrier, G., van den Besselaar, E.J.M., Jones, P.D., 2018. An ensemble version of the E-OBS temperature and precipitation data sets. *J. Geophys. Res.: Atmos.* 123 (17), 9391–9409.
- De Luca, P., Hillier, J., Wilby, R., Quinn, N., Harrigan, S., 2017. Extreme multi-basin flooding linked with extra-tropical cyclones. *Environ. Res. Lett.* 12.
- Easterling, D.R., Meehl, G.A., Parmesan, C., Changnon, S.A., Karl, T.R., Mearns, L.O., 2000. Climate extremes: observations, modeling, and impacts. *Science* 289 (5487), 2068–2074.
- Environmental Agency, 2016. The costs and impacts of the winter 2013 to 2014 floods. The UK government, Project Summary SC140025t.
- Fink, A.H., Brücher, T., Ermert, V., Krüger, A., Pinto, J.G., 2009. The European storm Kyrill in January 2007: synoptic evolution, meteorological impacts and some considerations with respect to climate change. *Nat. Hazards Earth Syst. Sci.* 9 (2), 405–423.
- Hawcroft, M., Dacre, H., Forbes, R., Hodges, K., Shaffrey, L., Stein, T., 2017. Using satellite and reanalysis data to evaluate the representation of latent heating in extratropical cyclones in a climate model. *Clim. Dynam.* 48, 2255–2278.
- Hawcroft, M.K., Shaffrey, L.C., Hodges, K.I., Dacre, H.F., 2012. How much northern hemisphere precipitation is associated with extratropical cyclones? *Geophys. Res. Lett.* 39 (24).
- Hersbach, H., Bell, B., Berrisford, P., Hirahara, S., Horányi, A., Muñoz Sabater, J., Nicolas, J., Peubey, C., Radu, R., Schepers, D., Simmons, A., Soci, C., Abdalla, S., Abellan, X., Balsamo, G., Bechtold, P., Biavati, G., Bidlot, J., Bonavita, M., De Chiara, G., Dahlgren, P., Dee, D., Diamantakis, M., Dragani, R., Flemming, J., Forbes, R., Fuentes, M., Geer, A., Haimberger, L., Healy, S., Hogan, R.J., Hólm, E.,

- Janisková, M., Keeley, S., Laloyaux, P., Lopez, P., Lupu, C., Radnoti, G., de Rosnay, P., Rozum, I., Vamborg, F., Villaume, S., Thépaut, J.-N., 2020. The ERA5 global reanalysis. *Q. J. R. Meteorol. Soc.*
- Hewson, T.D., Neu, U., 2015. Cyclones, windstorms and the IMILAST project. *Tellus* 67 (1), 27128.
- Hodges, K.I., 1994. A general method for tracking analysis and its application to meteorological data. *Mon. Weather Rev.* 122 (11), 2573–2586.
- Hodges, K.I., 1995. Feature tracking on the unit sphere. *Mon. Weather Rev.* 123 (12), 3458–3465.
- Hodges, K.I., 1999. Adaptive constraints for feature tracking. *Mon. Weather Rev.* 127 (6), 1362–1373.
- Hoskins, B.J., Hodges, K.I., 2002. New perspectives on the northern hemisphere winter storm tracks. *J. Atmos. Sci.* 59 (6), 1041–1061.
- Martius, O., Pfahl, S., Chevalier, C., 2016. A global quantification of compound precipitation and wind extremes. *Geophys. Res. Lett.* 43 (14), 7709–7717.
- National Climatic Data Center, 2018. Global Surface Summary of the Day. National Climatic Data Center, NESDIS, NOAA, U.S. Department of Commerce, <https://catalog.data.gov/dataset/global-surface-summary-of-the-day-gsod>.
- Pall, P., Aina, T., Stone, D.A., Stott, P.A., Nozawa, T., Hilberts, A.G., Lohmann, D., Allen, M.R., 2011. Anthropogenic greenhouse gas contribution to flood risk in England and Wales in autumn 2000. *Nature* 470 (7334), 382.
- Perkins-Kirkpatrick, S., Pitman, A., Holbrook, N., Mcaneney, J., 2007. Evaluation of the AR4 climate models' simulated daily maximum temperature, minimum temperature, and precipitation over Australia using probability density functions. *J. Clim.* 20.
- Pfahl, S., 2014. Characterising the relationship between weather extremes in Europe and synoptic circulation features. *Nat. Hazards Earth Syst. Sci.* 14 (6), 1461–1475.
- Pfahl, S., Wernli, H., 2012. Quantifying the relevance of cyclones for precipitation extremes. *J. Clim.* 25 (19), 6770–6780.
- Raveh-Rubin, S., Wernli, H., 2015. Large-scale wind and precipitation extremes in the Mediterranean: a climatological analysis for 1979–2012. *Q. J. R. Meteorol. Soc.* 141 (691), 2404–2417.
- Raveh-Rubin, S., Wernli, H., 2016. Large-scale wind and precipitation extremes in the Mediterranean: dynamical aspects of five selected cyclone events. *Q. J. R. Meteorol. Soc.* 142 (701), 3097–3114.
- Ridder, N.N., Pitman, A.J., Westra, S., Ukkola, A., Do, H.X., Bador, M., Hirsch, A.L., Evans, J.P., Di Luca, A., Zscheischler, J., 2020. Global hotspots for the occurrence of compound events. *Nature Commun.* 11 (5956).
- Roberts, J.F., Champion, A.J., Dawkins, L.C., Hodges, K.I., Shaffrey, L.C., Stephenson, D.B., Stringer, M.A., Thornton, H.E., Youngman, B.D., 2014. The XWS open access catalogue of extreme European windstorms from 1979 to 2012. *Nat. Hazards Earth Syst. Sci.* 14 (9), 2487–2501.
- Swiss Re, 2000. Storm over Europe – An underestimated risk. Swiss Re publishing, Zurich, p. 27.
- Tout, D.G., Kemp, V., 1985. The named winds of Spain. *Weather* 40 (10), 322–329.
- Van Den Besselaar, E.J.M., Klein Tank, A.M.G., Van Der Schrier, G., Abass, M.S., Baddour, O., Van Engelen, A.F., Freire, A., Hechler, P., Laksono, B.I., Iqbal, Jilderda, R., Foamouhoue, A.K., Kattenberg, A., Leander, R., Güingla, R.M., Mhanda, A.S., Nieto, J.J., Sunaryo, Suwondo, A., Swarimoto, Y.S., Verver, G., 2015. International climate assessment & dataset: Climate services across borders. *Bull. Am. Meteorol. Soc.* 96 (1), 16–21.
- Waliser, D., Guan, B., 2017. Extreme winds and precipitation during landfall of atmospheric rivers. *Nat. Geosci.* 10:1752–0908.
- Zscheischler, J., Westra, S., Hurk, B., Seneviratne, S., Ward, P., Pitman, A., AghaKouchak, A., Bresch, D., Leonard, M., Wahl, T., Zhang, X., 2018. Future climate risk from compound events. In: *Nature Climate Change*.